



Poster Abstracts: Congenital Heart Disease

315. Myocardial Injury After Percutaneous Transluminal Septal Myocardial Ablation in Hypertrophic Obstructive Cardiomyopathy: Evaluation by Magnetic Resonance Imaging

Willem G. van Dockum,¹ Folkert J. ten Cate, MD, PhD,² Jurrien M. ten Berg, MD, PhD,³ Aernout M. Beek, MD,¹ Jos W. R. Twisk, PhD,⁴ Mark B. M. Hofman, PhD,⁵ Cees A. Visser, MD, PhD,¹ Albert C. van Rossum, MD, PhD.¹
¹Cardiology, VU University Medical Center, Amsterdam, Netherlands, ²Cardiology, Thoraxcenter Erasmus Medical Center, Rotterdam, Netherlands, ³Cardiology, St. Antonius Hospital, Nieuwegein, Netherlands, ⁴Clinical Epidemiology and Biostatistics, VU University Medical Center, Amsterdam, Netherlands, ⁵Clinical Physics and Informatics, VU University Medical Center, Amsterdam, Netherlands.

Introduction: Percutaneous transluminal septal myocardial ablation (PTSMA) reduces left ventricular outflow tract (LVOT) obstruction in patients with symptomatic hypertrophic obstructive cardiomyopathy (HOCM).

Purpose: The purpose of the study was to evaluate myocardial injury induced by PTSMA using cine and contrast-enhanced magnetic resonance imaging (MRI).

Methods: Twenty-four patients (age 52 ± 15 years) underwent MRI before and 1 month after PTSMA. Cine MRI was performed for assessment of LV function and mass, and contrast-enhanced (gadolinium-DTPA) delayed inversion-recovery prepared gradient-echo MRI for assessment of PTSMA induced myocardial injury size. Hyperenhanced myocardium was quantified and compared to volume of alcohol administered, peak enzyme release, and reduction of the LV outflow tract gradient.

Results: After PTSMA total LV myocardial mass decreased from 219 ± 64 to 205 ± 64 g ($p < 0.001$), and septal mass from 76 ± 25 to 68 ± 22 g ($p < 0.001$). All

patients demonstrated regional myocardial hyperenhancement of the interventricular septum, exclusively located on the right ventricular side of the septum in 7. Hyperenhanced myocardium amounted to 20 ± 9 g (range: 5–41), corresponding to $10 \pm 5\%$ and $31 \pm 16\%$ of total LV and septal mass respectively. Injury size significantly correlated with the volume of ethanol administered ($\beta = 0.47$, $p = 0.02$), peak CK-MB ($\beta = 0.67$, $p = 0.001$), and reduction of the LV outflow tract gradient ($\beta = 0.63$, $p = 0.002$).

Conclusions: In patients with HOCM, size and location of myocardial injury induced by PTSMA can be determined using contrast-enhanced MRI. Injury size correlates with the volume of ethanol administered, peak enzyme release and reduction of the LV outflow tract gradient.

316. Quantitative Analysis of Regional Systolic Function in Hypertrophic Cardiomyopathy with Gadolinium Enhancing Abnormalities

Anthony H. Aletras, Ph.D., Kwabena O. Agyeman, M.D., Wiphada P. Ingkanisorn, M.D., Lameh Fananapazir, M.D., Andrew E. Arai, M.D. *National Heart, Lung and Blood Institute, National Institutes of Health, Bethesda, MD, USA.*

Introduction: Two distinct patterns of gadolinium enhanced T1 myocardial imaging have been identified in patients with hypertrophic cardiomyopathy (HCM). Distinct hyperenhancement (**Hyper**) in HCM demonstrates myocardial signal intensity comparable to that of the LV blood pool and also qualitatively appears similar to regions of myocardial infarction seen in patients with coronary artery disease. An intermediate degree of enhancement (**Inter**) has also been observed in patients

with HCM. Inter areas are of a signal intensity that is less than Hyper but also is higher than that of normal myocardium. These two patterns of gadolinium enhancement may be the result of myocardial infarction or fibrosis. Since delayed enhancement is associated with myocardial viability, we studied the functional performance of the myocardium of patients with HCM based on the observed patterns of gadolinium enhancement. DENSE is functional MRI method that stands for Displacement ENcoding with Stimulated Echoes. Displacement of tissue is encoded in the phase of the image allowing automatic analysis of regional contractile function at high resolution.

Purpose: The purpose of this study was to quantify regional systolic strain with DENSE in order to ascertain if different degrees of gadolinium enhancement are associated with graded abnormalities in myocardial function.

Methods: Twenty-two patients with known or suspected HCM were imaged. Regional left ventricular systolic strain was quantified using a rapid imaging variant of DENSE i.e. meta-DENSE. Imaging parameters were: encoding interval equal to systole, bandwidth ± 31.25 kHz, 2.8×2.8 mm² in-plane resolution, acquisition time of 14 heartbeats, displacement encoding of 2.0 mm/ π , slice 8 mm, echo train length 24, and acquisition window 108 ms. Myocardial gadolinium enhancement was imaged approximately 20 minutes after 0.2 mmol/kg Gd-DTPA using phase sensitive inversion recovery gradient recalled echo (PSIR-GRE). PSIR-GRE parameters were: TI approx. 300 ms, bandwidth ± 31.25 kHz, TE = 3.4 msec, TR = 7.8 msec, flip 20°, matrix 256×96 , FOV 360×270 , 8 mm slice thickness, 12 views per segment, acquisition time of 16 heartbeats. Cardiac anatomy and qualitative function were also imaged with steady state free precession (SSFP). Signal intensity average values were measured for normal myocardium (Normal), blood and noise (Air) along with measurements taken inside the lesions (Hyper or Inter). Signal-to-noise ratio (SNR) was calculated. To preserve sample independence, Hyper and Inter measurements were taken into account only once per patient even though multiple such regions may have existed in a given patient. Circumferential Shortening (CS) and Radial Thickening (RT) DENSE measurements were made for myocardium characterized as Normal, Hyper and Inter. All values reported are mean \pm SD. Two-tailed paired student's t-tests were used to determine statistical significance.

Results: Nineteen of 22 patients with HCM had gadolinium enhanced abnormalities. The Hyper pattern

was found in 6 patients, the Inter in 9 while 4 patients exhibited both patterns. The signal to noise ratios were: Hyper 34.5 ± 14 , Blood 36.5 ± 13.9 , Inter 10.5 ± 3.7 , Normal 5.6 ± 1.3 . Hyper regions had significantly higher SNR than Inter ($p < 0.001$) and Normal ($p < 0.001$) while there were not significantly different than Blood ($p = 0.196$). Inter regions had SNR intermediate to those of Hyper and normal myocardium. Inter regions were significantly different than Blood ($p < 0.001$) and Normal ($p < 0.001$). Regional systolic strain was abnormal for both Hyper and Inter type myocardium compared with normal myocardium. CS was 0.05 ± 0.02 , 0.07 ± 0.04 , and 0.25 ± 0.06 for Hyper, Inter, and normal myocardium respectively. Similarly, RT was 0.06 ± 0.02 , 0.08 ± 0.03 , and 0.25 ± 0.06 for Hyper, Inter, and normal myocardium. DENSE data show that Normal CS and RT are significantly different than those of either Hyper or Inter (all $p < 0.001$). Function in Hyper and Inter regions was not significantly different (CS: $p = 0.41$, RT $p = 0.76$).

Conclusions: Automatic quantitative analysis of regional contractile function found systolic functional abnormalities in patients with HCM as measured with high-resolution DENSE. Delayed hyper-enhancement findings can be stratified in two categories of distinct hyperenhancement (Hyper) and intermediate (Inter) lesions. Both categories of gadolinium enhancement exhibited similar degrees of contractile deficits. DENSE also identified two patients with functional deficits where no delayed hyperenhanced lesions were detectable. Although even subtle contrast enhancement is associated with abnormal systolic strain, contractile abnormalities can also be seen in non-contrast enhanced myocardium in patients with HCM.

317. Role of Contrast-Enhanced MRA in the Diagnosis of Adult Patients with Multiple Aorto-Pulmonary Collateral Arteries and Partial Anomalous Pulmonary Venous Drainage

Sanjay K. Prasad, MD,¹ Nikolaos Soukias, MD,² Tim Hornung, MD,² Anitha Varghese, MBBS,¹ Dudley J. Pennell, MD,¹ Michael Gatzoulis, MD,² Raad H. Mohiaddin, PhD, FRCP.¹ ¹CMR Unit, Royal Brompton Hospital, London, United Kingdom, ²Adult Congenital Heart Unit, Royal Brompton Hospital, London, United Kingdom.

Introduction: Cardiovascular Magnetic Resonance (CMR) has an established role in the management of

patients with congenital heart disease. However, its application in the diagnosis of vascular anomalies such as multiple aorto-pulmonary collateral arteries (MAPCAs) and anomalous pulmonary venous drainage (APVD) remains limited. Breath-hold magnetic resonance angiography (CE-MRA) provides a minimally invasive technique to demonstrate these abnormalities in adult patients.

Purpose: We assessed the accuracy of CE-MRA using gadolinium-DTPA contrast agent in the detection of MAPCAs and APVD as an alternative to cardiac catheterisation.

Methods: CMR was undertaken with a 1.5 T Siemens Sonata scanner in 29 consecutive patients with a diagnosis of MAPCA (n = 16) or PAPVD (n = 13) made by echo, cardiac catheterization, or surgical inspection. (Typical parameters used were echo time 1.04 ms; TR—2.6 ms; flip angle 25°, matrix size—512 × 256; slice thickness—1.5 mm; FOV—30 × 40 cm; receiver bandwidth 700 Hz per pixel; acquisition time 14 to 32 s with one signal average; K-space filling was sequential).

Results: The mean age was 45 yrs (range 16–75 years) with 16 males. In both types of pathology, there was complete correlation compared with cardiac catheterisation, echo or surgical inspection (100% sensitivity and specificity). Additional information was gained for patients with MAPCAs on confluence and size of pulmonary arteries (14/16 [87.5%] had central arteries). CE-MRA was useful in the detection of pulmonary artery stenosis (n = 3), aneurysmal dilatation of pulmonary artery (n = 1) and additional anomalous vascular abnormality (n = 3). Shunt assessment where present (8/16) showed patency in all cases (100%). For adults with PAPVD, further information was obtained on drainage origin (n = 11). There were no complications.

Conclusions: Thus CMR incorporating 3D gadolinium-enhanced MRA provides a fast, non-invasive, radiation-free method of accurate delineation of MAPCAs and APVD in adult patients.

318. Right Ventricular Arrhythmias: Is There a Correlation Between Magnetic Resonance Imaging and Electrophysiologic Findings?

Thorsten Dill,¹ Okan Ekinci,² Ruzica Maksimovic,² Christian Reiner,² Georg Bachmann,² Christian Hamm,² Heinz-Friedrich Pitschner.² ¹Cardiology, Kerckhoff Heart Center, Bad Nauheim, Germany, ²Kerckhoff-Heart Center, Bad Nauheim, Germany.

Introduction and purpose: Right ventricular (RV) arrhythmias have been increasingly found in young patients. Since the diagnostic value of magnetic resonance imaging (MRI) in these patients has not been well established, the aim of the study was to assess correlation between MRI and electrophysiological findings.

Patients and Methods: The study group included 307 pts, 51.1% males (157/307), mean age 42.7 ± 15.2 years, who were referred for clinical evaluation of RV arrhythmia. All patients underwent clinical examination, electrophysiologic study, echocardiography and MRI. MRI findings were abnormal in 53 (17.3%) patients and included 17 (32.1%) patients with ARVC, 15 (28.3%) patients with idiopathic RV outflow tachycardia, 13 (24.5%) patients with polymorphic VES, and 8 (15.1%) patients with idiopathic VF.

Results: Fatty replacement was seen exclusively in the ARVC patients. Severe RV dilatation, RV aneurysm, prominent trabeculae, mild RV dilatation, RV wall motions abnormalities and segmental RV dilatation were seen more often in patients with ARVC than in other groups. Furthermore, there was statistically significant correlation among prolonged QRS complex (≥ 100 ms) and mild RV dilatation (p < 0.05), severe RV dilatation (p < 0.05), RV aneurysm (p < 0.05) and RV regional wall motion abnormalities (p < 0.01). Also, RV aneurysm correlated with RV VES (p < 0.05) and presence of sustained RV tachycardia (p < 0.05).

Conclusions: Functional and morphological abnormalities seen on MRI are more frequent in the ARVC patients. Additionally, there is significant correlation among MRI and electrophysiological data which could direct further clinical decision making in these patients.

319. Diagnostic Value of Magnetic Resonance Imaging in Patients with Atrial Septal Defect in Comparison to Heart Catheterization and Transesophageal Echocardiography

Thorsten Dill,¹ Thomas Neumann,² Okan Ekinci,² Michael Weber,² Matthias Rau,² Roland R. Brandt,² Christian W. Hamm.² ¹Cardiology, Kerckhoff Heart Center, Bad Nauheim, Germany, ²Kerckhoff Heart Center, Bad Nauheim, Germany.

Introduction: The defect diameter, shunt volume and size of right atrium (RA) and right ventricle (RV) are essential data for planning transcatheter closure of an atrial septal defect (ASD). Although, balloon sizing of

the defect on heart catheterization (HC) is still mandatory, and transesophageal echocardiography (TEE) is widely used as noninvasive imaging technique, magnetic resonance imaging (MRI) may play an important role in pre- and postprocedural evaluation of these patients.

Purpose: Therefore, we assessed the diagnostic value of MRI in the evaluation of size defect, shunt volume and RV diameters in comparison to HC and TEE.

Patients and Methods: 60 patients, male 30% (18/60), average age 44.3 ± 15.7 (range 15–74 years) with an ASD II were enrolled. They underwent TEE, HC and MRI (1.5T Siemens Vision or Sonata system). A Flash 2D cine GRE sequence (TR 60 ms, TE 5 ms, slice 6 mm) and a TrueFISP cine sequence (TR 32 ms, TE 1.6 ms, slice 5 mm) were used. On MRI Qp/Qs was calculated and compared to the HC Qp/Qs ratio. Defect size measurements of different techniques were compared. Investigators were blinded to the results of the other techniques.

Results: Qp/Qs ratio on baseline MRI examination was 1.56 ± 0.29 (range 1.05–2.2) while on HC 1.71 ± 0.30 (range 1.2–2.4). Correlation was statistically significant ($r = 0.65$, $p < 0.01$).

Defect size on MRI was 15.3 ± 7.4 mm (range 3–30 mm), on TEE 14.3 ± 4.9 mm (range 4–24 mm), and the balloon stretched diameter on HC was 23.4 ± 4.2 mm (range 14–32 mm). Correlation between defect size as on MRI vs TEE was ($r = 0.67$, $p < 0.01$), MRI vs HC ($r = 0.77$, $p < 0.01$), respectively. Linear regression equation for prediction the defect size on heart catheterization based on MRI is as follows ($R = 0.77$, $R^2 = 0.59$, $F = 38.1$, $p < 0.01$): $y = 14.9 + 0.6 \times \text{MRI defect size}$. A significant reduction of RV volumes and size after occlusion could be demonstrated.

Conclusions: Thus, MRI proved to be an accurate diagnostic tool in pre and post interventional assessment of ASD patients with transcatheter occlusion. These data indicate that MRI allows complete noninvasive assessment of morphological and hemodynamic parameters in these patients without radiation and only minimal patient discomfort.

320. Identification of Hypertrophic Cardiomyopathy by Magnetic Resonance Imaging in the Absence of Echocardiographic Diagnosis

Carsten Rickers, MD,¹ Norbert Wilke, MD,² Michael Jerosch-Herold, PhD,² Susan Casey, RN,³ John Wegner,²

Prasad Panse, MD,² Jochen Weil, MD,¹ Ravi Seethamraju, PhD,² Neeta Panse, MD,² Barry Maron, MD.³ ¹*Pediatric Cardiology, University Hospital Eppendorf, Hamburg, Germany,* ²*Radiology, cardiac MR, University of Minnesota, Minneapolis, MN, USA,* ³*Hypertrophic Cardiomyopathy Center, Minneapolis Heart Institut and Foundation, MN, USA.*

Introduction: The two-dimensional echocardiogram (ECHO) has been the standard, noninvasive diagnostic test for the clinical diagnosis of hypertrophic cardiomyopathy (HCM) and also has an important role in risk stratification. A direct relation between magnitude of wall thickness and risk for sudden death has been demonstrated. We hypothesized that MRI would be more powerful than echo in establishing the diagnosis and measuring the extent of hypertrophy in HCM. *Methods:* Forty-nine patients (age: 34 ± 16) suspected of (or known to have) HCM were imaged by both ECHO and MRI. With cine imaging 10–15, short axis slices (5–8 mm) were acquired to assess LV wall thickness. Standard LV cross-sectional views were obtained by Echo and compared to MRI. Maximum wall thickness was measured in 8 anatomic segments (anterior and posterior ventricular septum; anterolateral and posterior free wall) in both the distal and proximal LV; a total of 392 segments were assessed in 49 patients. Wall thickness measurements were made in a blinded fashion with ECHO and MRI. *Results.* In 3 of 49 pts (6%) with a family history of HCM, Echo was judged normal without LV hypertrophy in any segment. However, MRI showed otherwise undetected hypertrophy in the anterolateral free wall (17 and 20 mm; twins age 14 and 19 mm; age 43) resulting in the phenotypic diagnosis of HCM for the first time and triggering implantation of cardioverter-defibrillator for primary prevention of sudden death in 2 of them. MRI more commonly showed the greatest LV thickness than did Echo (26 vs 16 pts; $p < 0.05$). Also, MRI identified LVH (undetected by echo) in 29 of 392 segments (7%) in 16 pts (33%). In 6 pts, echo was technically suboptimal and MRI made the diagnosis of HCM in (3 pts) or excluded it (3 pts).

Conclusion: MRI was advantageous over ECHO to: 1) definitively identify regions of LV hypertrophy not recognized by ECHO, and therefore was solely responsible for the identification of the phenotype in 6% of pts; 2) enhance assessment of the magnitude of LV hypertrophy for the purpose of risk stratification and provide a diagnostic alternative for pts with technically inadequate Echo.

**321. Direct vs Indirect Measurement of Atrial Septal Defect (ASD) Flow by Retro-gated Velocity Encoded CMR**

Louise E. J. Thomson, MBChB, J. Kevin Harrison, MD, Anja Wagner, MD, Heiko Mahrholdt, MD, John F. Heitner, MD, Robert M. Judd, MD, Raymond J. Kim, MD. *Duke Cardiovascular MR Center, Duke Medical Center, Durham, NC, USA.*

Background: Pulmonary/systemic flow ratios (Qp/Qs) can be accurately measured by CMR when compared to invasive study (CATH). ASD flow can be calculated by subtracting systemic from pulmonary flow (INDIRECT). Direct visualization of ASD size and position is useful in planning Amplatzer device closure and allows measurement of net shunt flow (DIRECT).

Purpose: To compare direct and indirect methods of ASD flow quantification by CMR, with the gold standard of CATH.

Method: Patients attending for Amplatzer device closure of symptomatic ASD underwent CMR (1.5T Magnetom Sonata, Siemens Medical). Retro-gated velocity encoded cine images (breath-hold, encoded velocity 100–150 cm/sec, TE 3.3 ms, Temporal resolution 40 ms, slice thickness 5 mm, flip angle 25°) were obtained at the ASD after localization by multiple long and short axis true-FISP cine images. Pulmonary and aortic flow was measured 1.5–2 cm above valvular level (encoded velocity 150–220 cm/sec). Flow analysis and ASD area measurements used ARGUS software and were blinded to CATH results.

Results: Initial data for 5 females (age 48–67, mean 57 yr) with symptomatic ASD are presented. There is close correlation ($r = 0.999$, $p = 0.001$) between left to right ASD flow (L/min) by CATH and by INDIRECT CMR. There is an equally close correlation between CATH and DIRECT CMR measurement of ASD flow ($r = 0.997$, $p < 0.001$). Qp/Qs by CMR (0.87–2.39) agrees with CATH (0.98–2.33), correlation $r = 0.996$, $p = 0.004$, slope 1.13. The size of the Amplatzer

occluder required for defect closure correlates with CMR measurement of ASD area (0.59–3.8 cm², $r = 0.995$, $p < 0.001$) and mean ASD diameter ($r = 0.979$, $p = 0.004$). Direct visualization of ASD was possible in all patients.

Conclusion: Direct ASD visualization with velocity-encoded images provides an accurate measure of the magnitude of the intracardiac shunt and aids in determining the size of the closure device required.

322. SENSE PVM—A Comparative Study with Regular Q-Flow

Srirama V. Swaminathan, Ph.D.,¹ Anthon R. Fuisz, MD,² Uzma Iqbal, MD,² Joseph R. Osborne, MD.² ¹*Clinical Science, Philips Medical Systems, N.A., Bothell, WA, USA,* ²*Cardiac MRI, Washington Hospital Center, Washington, DC, USA.*

Introduction: Phase velocity mapping (pvm) sequences can be used to accurately measure blood flow in the aorta but are relatively time consuming. SENSitivity Encoding (SENSE) has been used successfully to improve acquisition time with other sequences.

Purpose: We hypothesized that SENSE-enhanced pvm could cut acquisition time without any loss in accuracy of volume measurements.

Methods: 5 patients undergoing pvm for clinical purposes were studied. All the measurements were performed on Philips Intera CV (Philips B.V., Nederland) system equipped with a 30 mT Master gradient system. SENSE enhanced pvm sequences were performed directly after standard pvm sequences. The Q-flow sequence used is a 2D Fast Field Echo (2D-FFE) with a TR/TE of 6.9/4.1 ms. A PC velocity of 250 cm/s was used and 2 signal averaging was done. The average time of acquisition was 3 minutes without SENSE and 1.5 minutes with SENSE. SENSE factor of 2 was used, with the same number of phases as the pvm sequence. Images were processed and volumes

Table 1.

	ASD flow CATH (L/min)	Indirect ASD flow MRI (L/min)	Direct ASD flow MRI (L/min)	ASD mean diameter (mm)	Amplatzer diameter (mm)
1	0.2	-0.16	-0.54	8.3	12
2	2.4	3.12	3.34	10	16
3	5.7	8.87	10.36	22.2	26
4	-0.2	-0.76	-0.65	8.8	12
5	5.0	Not obtained	9.09	19.4	26

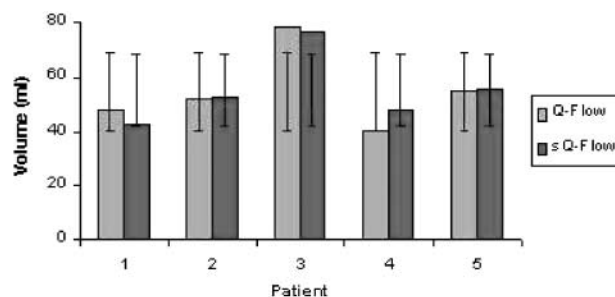


Figure 1. Bar chart comparing flow volumes from SENSE & non-SENSE measurement.

were calculated using Philips' Q-flow/S-track processing tool.

Results: Statistical analyses of the data from the two methods were done. The correlation coefficient was 0.956 suggesting a good correlation between the two methods. The average difference was about 0.5 ml with SENSE based method overestimating the volume compared to non-SENSE method. A bar chart comparing the flow volumes from the two methods are shown in Fig. 1. The error is less than 1-standard deviation.

Conclusions: SENSE based Q-flow method cuts the total acquisition time by a factor of 2 as hypothesized and compares well to non-SENSE based method. With SENSE one can acquire more phases, hence an increased temporal resolution without any penalty in acquisition time.

323. Aortic Elasticity in Marfan Patients with and without Aortic Root Replacement

Gijs J. Nollen,¹ Lilian J. Meijboom,² Maarten Groenink,² Naeem Merchant,³ Gary D. Webb,³ Ernst E. van der Wall,⁴ Barbara J. M. Mulder.² ¹Cardiology, Academic Medical Center, Amsterdam, Netherlands, ²Academic Medical Center, Amsterdam, Netherlands, ³The Toronto Hospital, Toronto, ON, Canada, ⁴Leiden University Medical Center, Leiden, Netherlands.

Introduction: Aortic elasticity is decreased in non-operated Marfan patients and has been related to aortic rupture behavior. In Marfan patients, aortic elasticity after aortic root replacement has not yet been investigated.

Purpose: Aim of the current study was 1) to investigate the feasibility of magnetic resonance (MR) imaging for the assessment of aortic elasticity in Marfan

patients after elective aortic root replacement, and 2) to compare aortic elasticity of Marfan patients with elective aortic root replacement with aortic elasticity of non-operated Marfan patients.

Methods: Thirty-nine Marfan patients (mean age 32 ± 11 years) with elective aortic root replacement and 78 Marfan patients without previous surgery (mean age 31 ± 8 years) underwent MR imaging. Aortic dimensions and elasticity were measured at 4 predefined levels in the aorta. Aortic elasticity, measured by means of local distensibility and regional flow wave velocity, was successfully assessed with MR imaging in all Marfan patients.

Results: No significant differences in aortic elasticity between Marfan patients with and without aortic root replacement were shown. In operated Marfan patients a positive correlation between age and flow wave velocity was demonstrated.

Conclusions: Our findings suggest that patients after elective aortic root replacement may not be at higher risk for aortic complications in the residual aorta than non-operated patients. Clinical follow-up studies are required to assess the prognostic significance of our findings.

324. Injury Size and Location Induced by Percutaneous Transluminal Septal Myocardial Ablation in Hypertrophic Obstructive Cardiomyopathy: Effect on Gradient Reduction

Willem G. van Dockum, MD,¹ Folkert J. ten Cate, MD, PhD,² Jurrien M. ten Berg, MD, PhD,³ Aernout M. Beek, MD,¹ Jos W. R. Twisk, PhD,⁴ Jeroen Vos, MD,² Mark B. M. Hofman, PhD,⁵ Cees A. Visser, MD, PhD,¹ Albert C. van Rossum, MD, PhD.¹ ¹Cardiology, VU University Medical Center, Amsterdam, Netherlands, ²Cardiology, Thoraxcenter Erasmus Medical Center, Rotterdam, Netherlands, ³Cardiology, St Antonius Hospital, Nieuwegein, Netherlands, ⁴Clinical Epidemiology and Biostatistics, VU University Medical Center, Amsterdam, Netherlands, ⁵Clinical Physics and Informatics, VU University Medical Center, Amsterdam, Netherlands.

Introduction: Percutaneous transluminal septal myocardial ablation (PTSMA) reduces left ventricular outflow tract (LVOT) obstruction in patients with symptomatic hypertrophic obstructive cardiomyopathy (HOCM).

Purpose: The aim of this study was to evaluate by contrast-enhanced magnetic resonance imaging (MRI)

the effect of myocardial injury size and location induced by PTSMA on LVOT gradient reduction.

Methods: Twenty-four patients (age 52 ± 15 years) underwent contrast-enhanced (gadolinium-DTPA) MRI 1 month after PTSMA for assessment of PTSMA induced myocardial injury size. Location of hyperenhanced myocardium was compared with ethanol infused target septal branch, site of balloon inflation and the volume of alcohol administered. Reduction of the LVOT gradient post PTSMA was determined by echocardiographic.

Results: All patients demonstrated regional myocardial hyperenhancement of the interventricular septum, exclusively located on the right ventricular side of the septum in 7. In patients with exclusively right sided hyperenhancement, the LVOT gradient reduction was 30 ± 28 mmHg versus 78 ± 22 mmHg in the remaining patients ($p < 0.001$). Myocardial injury size in the right sided group was significantly lower (10 ± 4 g vs. 23 ± 8 g, $p < 0.001$). In these patients the volume of ethanol injected was lower (2.6 ± 1.2 ml versus 3.6 ± 1.8 ml, $p = 0.19$) and the ethanol was infused distal of a bi- or trifurcation in 4 out of 7 patients. In the remaining patients ethanol was injected proximally in the septal branch.

Conclusions: In patients with HOCM, size and location of myocardial injury induced by PTSMA can be determined using contrast-enhanced MRI. An exclusively right sided location of myocardial injury is associated with lesser reduction of the LVOT gradient.

325. Differences in Collateral Flow Before and After Surgical Repair of Coarctation of the Aorta Examined by Magnetic Resonance Imaging

Salil J. Patel,¹ Pei-Hsiu Huang, BS,² John Oshinski, PhD,² W. James Parks, MD,³ Marijn E. Brummer, PhD,² Josh Socolow, MD,¹ Roderic I. Pettigrew, MD, PhD.²

¹Department of Medicine (Cardiology), Emory University, Atlanta, GA, USA, ²Department of Radiology, Emory University, Atlanta, GA, USA, ³Sibley Heart Center Cardiology, Children's Healthcare of Atlanta, Atlanta, GA, USA.

Introduction: Patients with long-standing coarctation of the aorta compensate for decreased aortic flow by the development of a collateral blood supply via thoracic vessels which drain into the descending aorta below the obstruction. Evaluation of such collateral flow may prove important to the changes in aortic wall stresses after surgical repair. Previous studies have measured collateral

flow non-invasively, by magnetic resonance (MR) imaging [1]. Steffans et al. found that in individuals with moderate to severe coarctation of the aorta, blood flow was increased at the diaphragmatic aorta as compared to the aorta immediately distal to the coarctation due to the presence of collateral blood flow. No study has quantitated whether augmented flow due to collateral blood flow persists after coarctation repair.

Purpose: The purpose of this study was to quantitate and compare multiple levels of descending aortic blood flow in patients before coarctation repair aorta to that in a group of patients after surgical coarctation repair.

Methods: Velocity encoded cine magnetic resonance imaging (VENC-MRI) was used to examine flow through three locations of the descending thoracic aortas in coarctation patients. There were thirty-seven patients, 18 having coarctation (pre-repair) and 19 after surgical repair. Pre-repair patients ranged in age from 1 to 18 years (median 6) and in the post-repair group ages ranged from 5 to 23 years (median 15). Two control groups were selected to match the mean age of either the pre-repair (control group A) or the post-repair group of patients (control group B). The three levels of the aorta that were evaluated were immediately below to the coarctation ("proximal"), at the level of the diaphragm ("distal"), and an area midway between the two these areas ("mid"). Data were analyzed by through-plane flow measurement using a program Flow (AZL, Lieden, The Netherlands) on a Sun Microsystems workstation.

Results: The thirty seven patients were analyzed as 2 groups; the 18 patients with coarctation of the aorta and 19 patients post-surgical repair, were similar except for their mean ages (coarctation = 9.3 ± 5.8 , post-surgery = 14.6 ± 4.1 ; $p < 0.05$). The two control groups had mean ages 10.0 ± 0.4 (Group A) and 14.3 ± 0.4 (Group B) years. The control groups did not significantly differ in mean age from their corresponding study group. Mid and distal flow results are reported as ratios referenced to flow in the proximal post-coarctation aorta. In the pre-repair group, the mid and distal flow ratio increased to 2.0 ± 1.1 ($p < 0.01$) and 1.9 ± 1.2 ($p < 0.01$) at the mid and distal aorta, respectively, relative to the proximal aorta. The post-surgery group had flow ratios of 1.11 ± 0.19 ($p = ns$) and 1.05 ± 0.18 ($p = ns$) at the mid and distal aorta, respectively, relative to the proximal aorta. Control group A had no significant change in flow ratios at the mid and distal aorta (mid = 0.97 ± 0.12 , distal = 0.97 ± 0.11 , $p < ns$). Control group B had a significant decrease in flow ratio at the distal aorta (mid = 0.98 ± 0.07 , distal = 0.84 ± 0.10 , $p < 0.05$).

Conclusion: Preoperatively patients had increased flow in the mid and distal aorta compared to

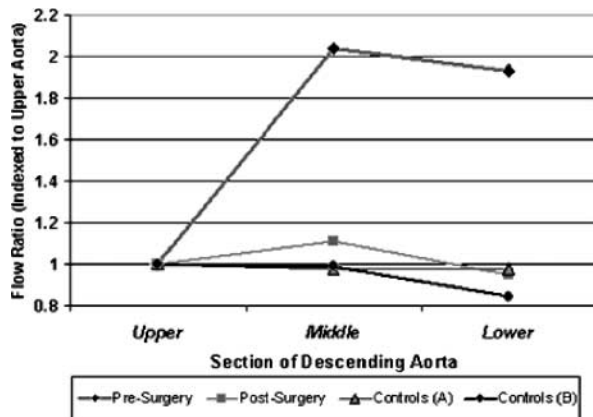


Figure 1. Collateral flow measurements.

the peri-coarctation zone due to the collateral flow. This increase was not present in post-op patients or in control groups.

References

1. Steffans, J.C. et al. *Circulation*. 1994; 90:937–943.

326. Left Ventricular Diastolic Biomechanics in Coarctation Using Magnetic Resonance Myocardial Tagging

Mark A. Fogel, MD,¹ Matthew Thomas,² Paul M. Weinberg, MD.² ¹*Pediatric Cardiology, Children's*

Hospital of Philadelphia, Philadelphia, PA, USA,
²*Children's Hospital of Philadelphia, Philadelphia, PA, USA.*

Introduction: Left ventricular (LV) diastolic biomechanics may play an important role in the pressure-overloaded LV. Little is known about the regional relaxation properties in this setting.

Purpose: To determine the homogeneity of LV regional wall relaxation and twist in the presence of pressure overload, using coarctation of the aorta as a model.

Methods: 23 patients with hemodynamically significant aortic coarctation underwent MRI diastolic myocardial tissue tagging using spatial modulation of magnetization through 3 short axis levels (base, mid region, and apex). Data was broken down into four anatomical regions from each slice level (superior, posterior, inferior and septal). Myocardial diastolic lengthening and thinning were measured. A fixed LV centroid was used for rotational analysis.

Results: There was uniform myocardial lengthening (circumferential dimension) and thinning (radial dimension) throughout all three short axis levels. Statistically significant differences in maximum rotation were found between both regional and slice level comparisons, with increasing rotation observed as the slice level progresses from base to apex. The regions from most to least rotation were superior, posterior, inferior, and septal (Fig. 1)

Conclusions: Diastolic biomechanics of the pressure-overloaded LV demonstrate uniform relaxation in

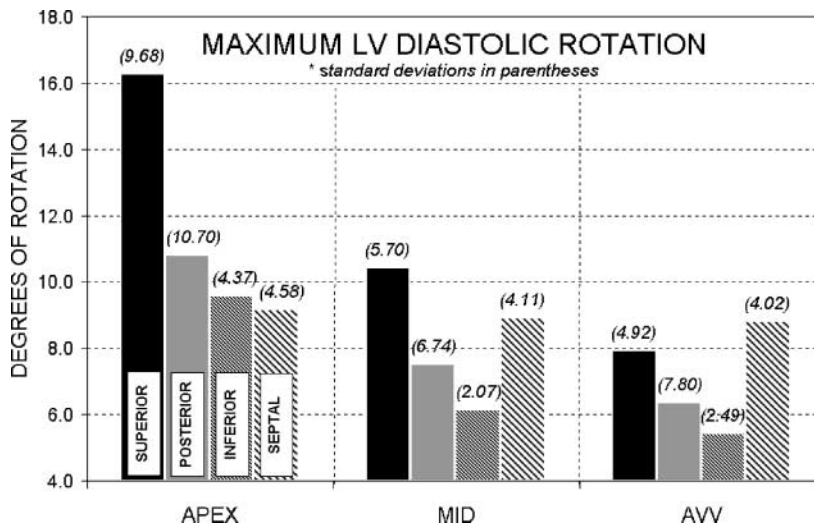


Figure 1.



the presence of heterogeneous rotation around the short axis. This data may lay the groundwork for therapeutic intervention.

327. Magnetic Resonance Imaging Evaluation of Airway Compression in Congenital Heart Disease

Alison L. Knauth, MD, PhD,¹ Andrew J. Powell, MD,¹ Lauren Senna, MD,² Tal Geva, MD.¹ ¹*Pediatric Cardiology, The Children's Hospital, Boston, Boston, MA, USA,* ²*Pediatric Radiology, The Children's Hospital, Boston, Boston, MA, USA.*

Objective: To determine the role of Magnetic Resonance Imaging (MRI) in evaluating airway compression in children with congenital heart disease (CHD), and to compare MRI to other, often more invasive imaging modalities.

Patients: A retrospective study of 30 children with CHD who were referred for MRI to evaluate symptoms of airway compression. Defects included 17 patients with vascular ring or arch abnormalities, 4 with tetralogy of Fallot and absent pulmonary valve, 3 with tetralogy of Fallot and pulmonary atresia, 2 with single ventricle, 2 with aortic stenosis, 1 with pulmonary atresia and intact ventricular septum, and 1 with D-transposition of the great arteries. Patient age ranged from 1 month to 49 years of age (14 were less than one year). Nine patients underwent catheterization, 22 had a CXR, 13 underwent bronchoscopy, 12 underwent UGI study, and 5 underwent CAT Scan. Twenty one patients underwent surgery to relieve the airway obstruction.

Methods: All patients were studied in a 1.5Tesla MRI scanner (Genral Electric) using 3D gadolinium enhanced MRA. General anesthesia was used in those patients unable to cooperate.

Results: MRI diagnosed significant airway compression in 26 of 30 patients. Airway compression was suggested by catheterization in 2 of 9 cases, by CXR in 9 of 22, by bronchoscopy in 12 of 13, by UGI in 11 of 12, and by CT Scan in 4 of 5. Except for CT Scan, only MRI was able to identify the mechanism of airway compression. The cause of airway compression was confirmed at surgery in all of the patients who underwent surgical correction of their airway compression.

Conclusions: MRI is a useful imaging modality for evaluating airway compression in children with CHD. MRI is noninvasive and does not employ ionizing radiation. MRI is able to accurately diagnose airway compression and uniquely determine the mechanism of compression.

328. Clinical Role and Technical Aspects of Cardiac MRI in Infancy

Beverly Tsai-Goodman,¹ Tal Geva,¹ Kirsten Odegard,² Lauren Sena,³ Andrew Powell.¹ ¹*Cardiology, Children's Hospital, Boston, MA, USA,* ²*Anesthesia, Children's Hospital, Boston, MA, USA,* ³*Radiology, Children's Hospital, Boston, MA, USA.*

Introduction: MRI has been demonstrated to be an important non-invasive diagnostic modality in patients with congenital heart disease; however, few studies have focused on young children.

Purpose: This study examined the clinical utility and technical challenges of cardiovascular MRI in infants.

Methods: All patients age <1year undergoing cardiac MRI at Children's Hospital Boston between January 1999 and July 2002 were identified and their MRI records and clinical data were retrospectively reviewed.

Results: A total of 82 MRI studies (63% inpatients) were performed in 76 patients at a median age of 102 days (range 1–358 days) and with a median weight of 5.0 kg (range 1.2–16.3 kg). All examinations were performed under general anesthesia using either a head (n = 48), cardiac (n = 18), shoulder (n = 13), or 5" surface (n = 3) RF receiver coil. No clinical decompensation or other complications occurred. Referral questions were pulmonary artery anatomy (n = 16), aortic anatomy (n = 11), vascular ring anatomy (n = 12), airway compression (n = 10), pulmonary venous anatomy (n = 10), cardiac tumor (n = 7), aorto-pulmonary collaterals (n = 4) and other (n = 12). Prior investigations for these questions included echocardiography (70%), cardiac catheterization (10%), bronchoscopy (7%), CT scan (2%), or TEE (1%). MRI provided the requested diagnostic information in all studies. Furthermore, in 15/82 (18%) examinations, MRI yielded an additional unsuspected diagnosis. Findings at surgery (n = 42) and cardiac catheterization (n = 10) were all concordant with those found by MRI. Systematic review demonstrated that airway anatomy was best shown with fast spin echo sequences and the thoracic vasculature by Gadolinium-enhanced 3DMR angiography.

Conclusion: Cardiac MRI is a useful and safe imaging modality in assessing thoracic vasculature and airway anatomy in infants with congenital heart disease. In some cases, it obviates the need for cardiac catheterization or bronchoscopy.

329. Rapid Left-to-Right Shunt Quantification in Children by Phase-Contrast MRI Using Sensitivity Encoding (SENSE)

Philipp B. J. Beerbaum, MD,¹ Hermann Körperich, PhD,¹ Jürgen Gieseke, MSc,² Peter Barth, MSc,¹ Herrmann Esdorn, MD,¹ Johannes Hartmann, MD,¹ Hans Meyer, MD.¹ ¹*Clinic for Congenital Heart Disease and Institute for Magnetic Resonance Imaging, Heartcenter NRW, Ruhr-University Bochum, Bad Oeynhausen, Germany,* ²*Philips Medical Systems, Best, Netherlands.*

Introduction: Phase-contrast MRI (PC-MRI) is feasible in children with cardiac left-to-right shunt but still time-consuming.

Purpose: To evaluate rapid PC-MRI techniques using sensitivity encoding (SENSE).

Methods: In 24 children (mean age 7.2 years, 13 girls) with cardiac left-to-right shunt, and in 12 healthy adult volunteers (mean age 32 years), blood flow rate in the pulmonary artery (Qp) and aorta (Qs) was determined by PC-MRI at 2 different in-plane resolutions (2.4*3.2 mm and 1.5*2.1 mm) with sensitivity encoding (PC-MRI/SENSE). Stroke volumes and Qp/Qs ratio were compared with results from a recently validated standard PC-MRI protocol using Bland-Altman analysis of agreement.

Results: For blood flow rate through the pulmonary artery and ascending aorta as well as for Qp/Qs ratio in the pediatric patients, we found mean

differences of 0–4%, and lower limits of agreement (mean-SD) of -7% to -12%, and upper limits of agreement (mean + SD) of +7 to +16%, demonstrating good agreement between PC-MRI/SENSE at different inplane resolutions and the standard PC-MRI protocol. We observed similar agreement in healthy adult volunteers. Qp/Qs was 1.69 (SD ± 0.45) in children and 1.04 (SD ± 0.07) in volunteers. In children, acquisition time for PC-MRI/SENSE sequences was 15–45 sec. depending on heart rate, spatial resolution and SENSE-factor, as opposed to 2.5–3.5 min. by standard cine PC-MRI. For all pulse sequences, interobserver agreement was good, and accuracy confirmed by in vitro experiments.

Conclusions: In children with cardiac left-to-right shunt, accurate Qp/Qs quantification is possible by PC-MRI/SENSE in <90 sec. as opposed to 5–7 minutes by standard PC-MRI.

330. Branch Pulmonary Artery Regurgitant Fraction: A New Index to Estimate the Relative Right and Left Pulmonary Vascular Resistances in Congenital Heart Disease

Matthew Harris, MD,¹ Paul M. Weinberg, MD,¹ Neha Kothari, MD,² Mark A. Fogel, MD.¹ ¹*Cardiology, Children's Hospital of Philadelphia, Philadelphia, PA, USA,* ²*Radiology, Children's Hospital of Philadelphia, Philadelphia, PA, USA.*

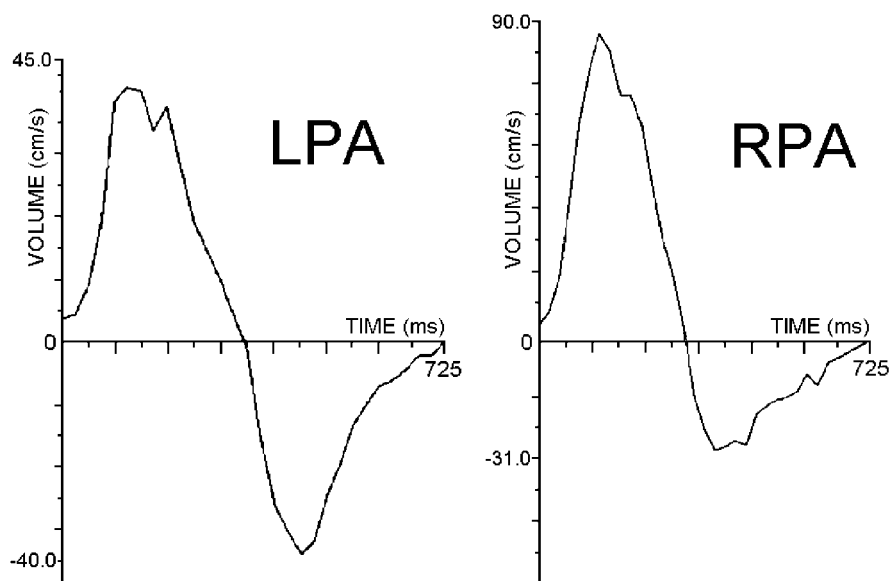


Figure 1. (Abstract 330)

Introduction: Patients with Tetralogy of Fallot (TOF) and D-Transposition of the Great Arteries (D-TGA) undergo surgical repair which can render their pulmonary valve incompetent resulting in pulmonary regurgitation (PR). In the absence of discrete stenosis or hypoplasia of the pulmonary arteries, the degree of PR in the branch pulmonary arteries is proportional to the distal pulmonary vascular resistance (PVR). We hypothesized that there should be equal regurgitation in both the right (RPA) and left (LPA) pulmonary arteries.

Purpose: To identify any existing differences in the regurgitant fraction (RF) between the branch pulmonary arteries.

Methods: We performed through-plane-phase-encoded velocity maps of the branch pulmonary arteries in 9 patients who had TOF (5) or D-TGA (4). All patients had PR noted in at least one of the branch pulmonary arteries. We then calculated the RF from the volume-time curves produced.

Results: The RF in the left pulmonary artery was significantly greater than the right ($25.0 \pm 13\%$ vs. $12.3 \pm 11\%$, $P < .01$). Two patients demonstrated regurgitation in the LPA alone.

Conclusions: Significant differences in the RF exist between the RPA and LPA. The greater RF in the LPA suggests elevated PVR relative to the right lung in these patients. This information may be helpful in determining therapeutic options for patients with various lesions such as those requiring lung transplantation or Fontan reconstruction.

331. Magnetic Resonance Imaging and the Diagnosis of Right Ventricular Dysplasia in Children: An Institutional Experience

Mark A. Fogel, MD,¹ Paul M. Weinberg, MD,² Larry Rhodes, MD.² ¹*Pediatric Cardiology, Children's Hospital of Philadelphia, Philadelphia, PA, USA,* ²*Children's Hospital of Philadelphia, Philadelphia, PA, USA.*

Introduction: Magnetic resonance imaging (MRI) has been demonstrated to be helpful in adults in the diagnosis of right ventricular (RV) dysplasia. Short of direct observation by surgery or autopsy, no gold standard exists. A comprehensive diagnostic criteria for this diagnosis by MRI includes right atrial and ventricular dilation, regional RV wall motion abnormalities, RV outflow tract ectasia and RV myocardial fatty infiltration.

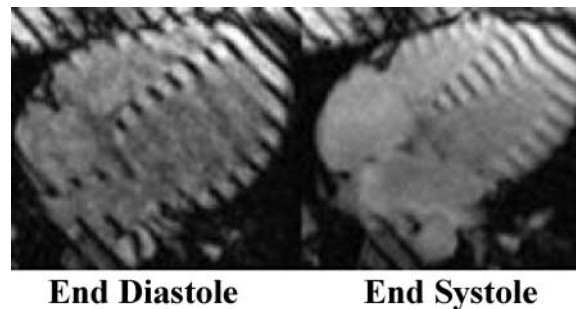


Figure 1.

Purpose: To determine whether these diagnostic criteria are useful in children referred to cardiac MRI with the suspicion of this diagnosis.

Methods: The images and records of 44 patients (ages 10.5 ± 4.7 years old) over an 7 year period from our institution were reviewed. Referral diagnoses included a history of ventricular tachycardia, palpitations, syncope, near sudden death or a family history of RV dysplasia. Four families were studied with parents who had RV dysplasia diagnosed by surgery, explanted heart, or MRI. MRI imaging included T1 weighted imaging in various views with and without fat saturation, cine MRI of the RV short axis, RV outflow tract and the 4 chamber view, 1-dimensional myocardial stripes of the RV myocardium, and phase encoded velocity mapping.

Results: None of the 44 patients met more than 2 of the criteria and only 2 patients met one or 2 criteria. For questionable regional wall motion abnormalities, one-dimensional myocardial tagging was able to identify normal myocardial shortening.

Conclusions: Cardiac MRI on patients with a history suspicious of the diagnosis of RV dysplasia is a low yield test in children. This may be due to evolving nature of the disease which does not manifest itself from a morphologic or ventricular function standpoint until later on in development. Follow-up studies as the patients age may be advantageous.

332. Quantifying Right Ventricular Regional Systolic Function: Tetralogy of Fallot Versus Normals Using MRI 1-D Myocardial Tagging

Jondavid Menteeer, MD, Paul M. Weinberg, MD, Mark Fogel, MD. *Cardiology, Children's Hosp of Philadelphia, Philadelphia, PA, USA.*

Introduction: Right ventricular (RV) function is notoriously difficult to quantify. Previous studies of

patients with Tetralogy of Fallot (TOF) have demonstrated decreased global systolic performance.

Purpose: To assess regional RV mechanics in both normals and in volume loaded TOF hearts.

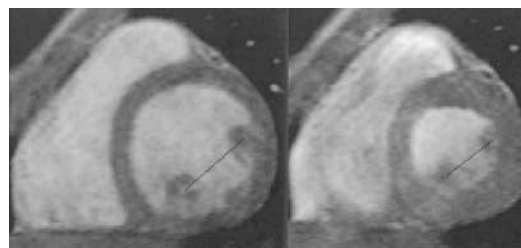
Methods: By performing 1-D tissue tagging perpendicular to the long axis in cine-MRI series in 4-chamber and RV long-axis views, we measured regional systolic shortening fractions (RSF's) of myocardium throughout the RV. We standardized twelve regions that can be assessed in these views, including three regions each along the RV free wall, the interventricular septum (IVS), the superior RV wall toward the outflow tract, and the inferior/diaphragmatic surface. The population included 13 normals and 6 patients with Tetralogy of Fallot (TOF) s/p transannular patch repair, ages 2 months to 16 years. Using computer-assisted intensity mapping, regional shortening was measured in each of the specified regions.

Results: In normals, areas with the smallest shortening fractions included the IVS near the atrioventricular canal (AVC) and the mid-IVS (20.5% and 18.1%). The most dynamic areas were the anterior free wall regions (near AVC 32%, mid 33.1%, apex 35.7%) and the mid- and apical-inferior wall (30.1% and 30.8%). These two groups were significantly different from one another (P 's all < 0.0002). The remaining regions had intermediate shortening, including the RV outflow tract (24.9%), inferior AVC (22.3%), superior midwall (28.2%), superior apex (26.6%), and septal apex (23.1%). TOF patients had significantly decreased shortening in all mid-free wall regions (superior, anterior, and inferior) as well as in the anterior apical region ($p < 0.05$).

Conclusions: Our preliminary data shows that RSF's can be measured in the RV using 1-D myocardial tagging. Areas of greatest fibrous tissue content such as the IVS and RV outflow tract tend to have the smallest RSF's, whereas free wall areas tend to have greater RSF's. TOF patients have decreased free wall shortening despite the volume load to their RV, consistent with previous studies of global ejection fractions in TOF.

333. Left Ventricular Papillary Muscle Mechanics in the Pediatric Heart: Insights Using Cine-Magnetic Resonance Imaging

Jondavid Mentee, Paul M. Weinberg, MD, Mark Fogel, MD. *Cardiology, Children's Hospital of Philadelphia, Philadelphia, PA, USA.*



Introduction: Previous investigations have shown that the left ventricle (LV), when viewed from the apex, twists counterclockwise at the apex, with relatively little rotation in either direction near the base.

Purpose: With this in mind, we sought to evaluate the mechanics of papillary muscles including their systolic twisting in the pediatric heart.

Methods: Cine-MRI images through the LV short axis at the midpapillary level were obtained. We analyzed papillary muscle twisting, interpapillary muscle shortening fraction (SF), and LV SF using end systolic and end-diastolic frames from studies on 19 normal children ages 18 months to 17.5 years (mean 9.8 years).

Results: The median twist of the LV papillary muscles during systole was 2 degrees clockwise (range +8 to -11 degrees). The average inter-papillary SF was $33\% \pm 7\%$, whereas the average LV SF was $37\% \pm 6\%$ ($P = \text{NS}$). No significant correlation existed between SF and degree of twisting or between patient age and degree of twisting. Measurement of angles using the centroid of a single papillary muscle versus the centroid of the entire papillary muscle complex made no difference to the measured degree of twist.

Conclusions: (1) The degree of papillary muscle twist in the normal pediatric patient varies considerably, but there is only a small median change. (2) No significant difference exists between interpapillary SF and traditional SF. (3) There is no correlation between SF and papillary muscle twist. This study lays the groundwork for evaluation of papillary muscle mechanics in congenital heart disease (Fig. 1).

334. MRI Pictorial Essay of Isolated Left Ventricular Non-compaction

Kurt Vanderdood, MD,¹ Ben Van Camp, MD,² Michel De Maeseneer, MD,¹ Michel Osteaux, MD.¹ *¹Radiology, Free University Brussels, AZ-VUB, Brussels, Belgium, ²Cardiology, Free University Brussels, AZ-VUB, Brussels, Belgium.*



Isolated left ventricular non-compaction (IVNC) was first described just over a decade ago and remains a rare cardiomyopathy, yet unclassified by the World Health Organization. The diagnosis in both children and adults is often overlooked although early detection and correct management of this condition are crucial as the clinical manifestation includes early heart failure (due to left ventricular dysfunction), life threatening ventricular arrhythmias and systemic embolic events.

IVNC is a genetically heterogeneous congenital disorder characterised by prominent myocardial trabeculations and deep intertrabecular recesses which lie in continuity with the left ventricular cavity. This condition results from an arrest of compaction of the loose interwoven meshwork of myocardial fibres during intrauterine life.

Jenni et al. established four echocardiographic morphological criteria diagnostic for IVNC:

- 1) Absence of coexisting cardiac anomalies.
- 2) A two layer structure is seen, with a compacted thin epicardial band and a much thicker non-compacted endocardial layer of trabecular meshwork with deep endocardial spaces. A maximal end systolic ratio of non-compacted to compacted layers of >2 is diagnostic.
- 3) The predominant localisation of the pathology is mid-lateral, apical and mid-inferior areas. Concomitant regional hypokinesia is not confined to the non-compacted segments.
- 4) Colour Doppler shows evidence of deep perfused intertrabecular recesses.

The purpose of this poster is to demonstrate that these four diagnostic criteria can be transferred to MRI, illustrated by comparing the echocardiographic images to the MR-images in the corresponding planes. High resolution static images clearly show the characteristic aspect of the ventricular wall. Functional examination (cine) demonstrates hypokinesia and intertrabecular blood-flow. Sequence parameters are extensively described.

The advantages of MRI on echocardiography, consisting in a better appreciation of the apex area and a more accurate visualization of possible thrombi, are emphasized.

335. Computer Stereolithography of Congenital Aortic Malformations Imaged by Magnetic Resonance

Khaled El-Said, BSE,¹ Howaida El-Said, MD, PhD,² Yasser Hosni, PhD,³ Raja Muthupillai, PhD,⁴ Ricardo H. Pignatelli, MD,² Taylor Chung, MD,⁵ Giles W. Vick,

III, MD, PhD.² ¹Industrial Engineering, University of Central Florida, Orlando, FL, USA, ²Pediatric Cardiology, Baylor College of Medicine, Houston, TX, USA, ³University of Central Florida, Orlando, FL, USA, ⁴Phillips Medical Systems, Bothell, WA, USA, ⁵Pediatric Radiology, Baylor College of Medicine, Houston, TX, USA.

Introduction: Direct physical examination is an excellent way to assess the complex spatial characteristics of congenital malformations of the aorta. However such direct physical evaluation has previously been feasible only at surgery and pathological examination. The development of new "biomodeling" engineering technology has facilitated production of plastic replicas from three dimensional computer datasets. This technology is known as rapid prototyping. Several processes can be utilized to form rapid prototypes, the most common being stereolithography. A stereolithography device effectively performs three dimensional printing by first electronically slicing computerized three dimensional model data into very thin cross sections. A small laser beam of ultraviolet light is then focused onto the surface of a vat of liquid photopolymer. When the laser beam strikes the photopolymer, a thin layer is turned to solid. The laser beam traces a cross section of the object to be constructed. Each thin cross section is then lowered and the succeeding section traced in an iterative manner until all sections have been scanned and the three dimensional object has been constructed.

Purpose: To determine the feasibility of using stereolithography to create plastic physical models of congenital malformations of the aorta from three dimensional magnetic resonance imaging (MRI) datasets.

Methods: Patients were imaged with standard MRI methods, including turbo spin echo, segmented multi-phasic gradient echo and gadolinium contrast enhanced angiography. Subsequent to acquisition of raw image data, aortas were segmented with computer assistance utilizing a combination of thresholding and seeding. A sequence of maximal intensity projections and surface rendered images were then generated and compared with the original MR images. Final surface renderings were approximated via straight lines and planes into tessellated facet format, the standard triangulation language interface. Layer thicknesses, intended building style, cure depths, hatch spacing, line width compensation value, and shrinkage compensation factors were then selected. Models were built with a stereolithography apparatus. Anatomic accuracy of the models were determined by comparison of electronic measurements

from MRI and physical measurements from the corresponding plastic stereolithography model.

Results: Physical replicas ($n = 10$) were manufactured from MRI studies of a normal aorta and of a variety of preoperative and postoperative congenital malformations of the aorta. Representations constructed included double aortic arch, native coarctation of the aorta, coarctation of the aorta status post repair with recurrent stenosis, coarctation of the aorta status post repair with aneurysm formation, right aortic arch with aberrant left subclavian artery, aortic atresia status post Norwood procedure, left aortic arch with aberrant right subclavian artery, right aortic arch with mirror image branching and anterior ductal ligamentum, and right aortic arch with mirror image branching and posterior ductal ligamentum. Models could readily be made from all types of MRI datasets, but segmentation was more rapid with gadolinium contrast enhanced datasets. Correlation between physical measurements made on the models and electronic measurements from MRI data was excellent.

Conclusion: 1. Stereolithography can create anatomically accurate plastic physical replicas of congenital malformations of the aorta from magnetic resonance imaging datasets.

2. These models are helpful as teaching aids and have many other potential uses in presurgical planning and in patient specific customization of stents and other intravascular devices.

336. Non-compaction Left Ventricle Versus Apical Cardiomyopathy. Role of Magnetic Resonance in Comparison with Echocardiography

Ana G. Almeida,¹ Claudio David, MD,² Monica M. Pedro, MD,² Eduardo I. Oliveira, MD,² Luis Sargento, MD,² Sandra Rodrigues,² M-Celeste Vagueiro, MD, PhD.² ¹Cardiology, University Hospital Santa Maria, Lisbon, Portugal, ²University Hospital Santa Maria, Lisbon, Portugal.

Introduction: Isolated left ventricular non-compaction is a recently identified cardiomyopathy, with prominent trabeculation of endocardium and associated with heart failure and thromboembolism. Diagnosis by transthoracic echocardiography is often missed.

Purpose: To assess the value of magnetic resonance (MR) in the differential diagnosis of apical LV non-compaction and apical cardiomyopathy, in comparison with transthoracic echocardiography (TTE).

Methods: We studied 9 patients (pts) with suspected diagnosis of apical non-compaction LV versus apical cardiomyopathy by TTE with harmonic imaging study. All were submitted to MRI and, subsequently, to transesophageal echocardiography (TEE), used as gold-standard. MRI study (GE, Signa 1.5T): high resolution spin-echo T1 (5 mm thick, 256×256 matrix, FOV 40–42) in the three long-axis views, breath-hold cine MR in the same planes, SE T1 with Gad DTPA. Intensity measurement of the apical region at the SE T1 sequence was compared to the one obtained at basal segments of LV.

Results: ETT identified one pt with LV non-compaction and another with probable diagnosis of this entity. MRI identified three pts with non-compaction of apical segments of LV and six with apical cardiomyopathy, excluding also the presence of thrombus or tumor. Those three pts had a two-layers structure of the myocardium, with prominent trabeculation of the endocardium, with visible flow in cine MR. TEE confirmed the diagnosis of LV non-compaction in these pts and the typical morphological pattern of apical cardiomyopathy in the remaining pts.

Conclusions: In the diagnosis of the non-compaction LV, MR was a reliable non-invasive method, comparable to ETE, a semi-invasive technique. Additionally, MR offers information on tissue characterization, such as the exclusion of thrombus or tumor.

337. Coarctation in Right Aortic Arch: A Rare Association

Fraz A. Ismat, M.D.,¹ Paul M. Weinberg, M.D.,¹ Jack Rychik, M.D.,¹ Tom R. Karl, M.D.,² Mark A. Fogel, M.D.¹ ¹Division of Cardiology, The Children's Hospital of Philadelphia, Philadelphia, PA, USA, ²Division of Pediatric Cardiothoracic Surgery, University of California, San Francisco, San Francisco, CA, USA.

Introduction: Coarctation of the aorta is a rare abnormality seen in patients with a functional right aortic arch (RAA).

Purpose: To determine the incidence of coarctation with RAA, and examine other anatomical and clinical correlates.

Methods: A retrospective review of our echocardiographic, MRI, and surgical databases was performed from 1988 to the present.

Results: Of 240 patients with RAA, 10 (4.1%) had coarctation which constituted 1.9% of all native

coarctations presenting to our institution. Interestingly, 9 (90%) had long segment hypoplasia. Five of the 10 (50%) RAAs had an aberrant left subclavian artery, 4 (40%) had mirror image branching, and 1 (10%) had a double aortic arch with atretic left arch. In addition, 6 (60%) had other congenital heart defects including 3 with ventricular septal defects, and one each with double outlet right ventricle, cor triatriatum, and pulmonary valve abnormality. None of the patients with long-segment hypoplasia had bicuspid aortic valve (BAV). Five (50%) had vascular rings, and 5 (50%) had associated syndromes including 2 with heterotaxy syndrome, 2 with Goldenhar's syndrome, and 1 with DiGeorge's syndrome. The combination of MRI and echocardiography successfully diagnosed all of these patients. Furthermore, although long segment RAA coarctation courses behind the trachea posteriorly, only 2 needed a jump graft; the remainders were repaired with patch angioplasty.

Conclusions: Coarctation with RAA is rare, constituting 4.1% of all patients with RAA, compared with 5–8% of patients with left aortic arch (LAA) and congenital heart disease. Nearly all had long segment hypoplasia, most of which could be repaired by patch angioplasty. There is no association with BAV (as in LAA), and half were part of other syndrome complexes. This association can be diagnosed noninvasively.

338. Isolated Subclavian Artery: Physiologic Diagnosis by Magnetic Resonance Pre-saturation Tagging

Mark A. Fogel, MD,¹ Paul M. Weinberg, MD.²
¹*Pediatric Cardiology, Children's Hospital of Philadelphia, Philadelphia, PA, USA,* ²*Children's Hospital of Philadelphia, University of PA School of Medicine, PA, USA.*

Introduction: Isolation of the subclavian arteries (ISA) can be both congenital as well as surgically induced. Blood is typically supplied to the ISA retrograde via

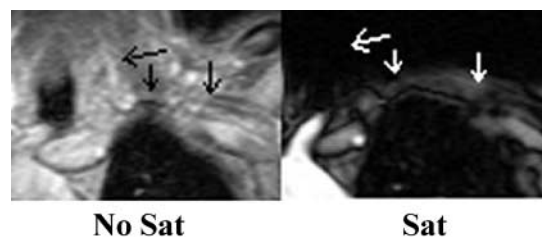


Figure 1.

the vertebral artery (VA). This can be difficult to visualize by echocardiography and in small children, may be difficult to determine anatomically by MRI. Although magnetic resonance imaging (MRI) using velocity mapping can delineate the direction of flow in the VA, this can be problematic in small children where not enough cross sectional area is present to obtain reliable data.

Purpose: To determine whether placing a pre-saturation pulse over the VA and imaging the ISA using gradient echo MRI can determine the direction of flow in all size children. This procedure destroys the spins in VA blood and should result in a loss of signal in the ISA.

Methods: We reviewed our experience with above pre-saturation pulse technique over a 6 year period in 6 patients with ISA (2 right and 4 left ISA). Patients with subclavian flap repair were excluded. The ISA and VA were imaged contiguously in the coronal plane using T1 weighted imaging via multiplanar reconstruction. A gradient echo sequence with and without a saturation pulse placed just above the VA–ISA junction was performed.

Results: In comparison with the gradient echo images without a pre-saturation band, the images with the pre-saturation band in all patients eliminated signal from the ISA, indicating retrograde flow in the VA supplying the ISA (Fig. 1).

Conclusions: Placing a pre-saturation pulse over the VA can aid in the physiologic diagnosis of ISA. This may be useful clinically if a “steal syndrome” is present or to diagnose subtle subclavian artery stenosis proximal to the VA–ISA junction.